FREQUENCY DOMAIN ANALYSIS OF EUROFIGHTER AERODYNAMICS

E. Özger,
EADS, Defence & Security – Military Air Systems
Rechliner Str, Manching
Germany

Abstract

This investigation deals with non-stationary effects in rolling and yawing moment just below and at maximum lift AoA for the Eurofighter aircraft, which is a delta-canard configuration. Spectral analysis of angle of attack, angle of sideslip, angular rates, flap deflections and rolling & yawing moment is performed where oscillations and the spectral content of rolling and yawing moment point to fluctuations of vortex breakdown location.

For all manoeuvres, the spectral content of the input variables (angle of attack, angle of sideslip, angular rates, flap deflections) is concentrated mainly below a Strouhal number of up to $Sr = fc/U_\infty < 0.04$ which is the typical frequency range for manoeuvring.

Preceding investigations in the literature on fluctuations in vortex breakdown location for slender and non-slender delta wings are confirmed. Fluctuations in the vortex breakdown location are reported to take place in a frequency range of around $0.05 < fc/U_\infty < 0.1$ which is far lower compared to the frequency range for helical mode or Kelvin-Helmholtz instabilities. It can be shown in this investigation that the relevant frequency range of $0.04 < fc/U_\infty < 0.14$ for rolling and yawing moment oscillations coincides with the frequency range of large amplitude fluctuations of breakdown location where the amplitude of oscillations depends on the manoeuvre type.

In contrast to preceding investigations, the structure of spectral content of rolling and yawing moment in this frequency range is rather complicated and multifaceted/multipeaked pointing to a multi modal three-dimensional movement of the various vortices of canard and wing leading edge and their breakdown locations on the wing.

1. SYMBOLS

ADM	aerodynamic model
AR	aspect ratio
b	wing span
c	reference cord
c_l	rolling moment coefficient
Δc_l	residual error rolling moment coefficient
c_m	pitching moment coefficient
c_n	yawing moment coefficient
Δc_n	residual error yawing moment coefficient
f	frequency in Hz
f_0	minimum frequency in Hz
f_1	maximum frequency in Hz
$f_{sampling}$	sampling frequency in Hz
FRD	frequency biased rudder doublet
FT	flight test
$\bar{\bar{I}}$	inertia matrix
$\vec{M}$	Moment vector
$\vec{M}_{FT}$	Moment vector of FT derived force
$\vec{M}_G$	Moment vector due to gravity
$\vec{M}_{Intake}$	Moment vector of intake force
$\vec{M}_{Nozzle}$	Moment vector of nozzle force
Ma	Mach number
p,q,r	roll, pitch, and yaw rate
q	dynamic pressure
PD	pitch doublet
R3211	3-2-1-1 type roll stick input
Re	Reynolds number
RR	rapid rolling
s	half span
S	reference wing area
$Sr = fc/U_\infty$	Strouhal number
T	time window of manoeuvre
U_∞	freestream velocity
WUT	wind-up turn
α_{max}, AoA_{max}	angle of attack at maximum lift
α, AoA	angle of attack
β, AoS	angle of sideslip
δ	flaperon deflection
Λ	leading edge sweep
ω_0	minimum frequency in rad/sec
ω_1	maximum frequency in rad/sec
$\vec{\omega}$	angular rate vector
ξ	aileron deflection
ζ	rudder deflection
$\Im$	functional

2. INTRODUCTION

The research of leading edge vortices of delta wings have always been a vivid field of interest. Much focus has been reserved for the flow over generic slender delta wings with a sharp leading edge whereas investigations on non-slender delta wings are relatively new. Like Hummel[9] many investigators can be mentioned who have thoroughly analysed the structure of the vortex flow field.

It is well known that slender delta wings produce a pair of primary vortices emanating from the wing leading edge

and contributing to the so-called non-linear vortex lift of the wing. Hummel[9] depicts very well potential flow and vortex flow contributions showing their effect on the circulation distribution on the delta wing.

Delta wing flow was originally associated with sharp leading edge geometries. The effect of other leading edge geometries is also relevant and it influences the flow differently. Luckring[11,12] shows for blunt leading edges that primary vortex separation is shifted from the apex/leading edge to a nearby region more towards the trailing edge depending on the leading edge geometry.

The flow is also different for non-slender delta wing configurations compared to slender delta wings. Elsayed et al.[3] show that the vortex flow has a different structure and has a higher sensitivity with respect to changes in angle of attack. Vortex breakdown is also known to reach the wing apex at much lower AoA for non-slender wings.

Taylor et al.[18] portray similarities and differences of the flow around slender and non-slender delta wings. Among the similarities are the formation of the inboard primary and the outboard secondary vortex due to induction. But the vortices over low sweep wings are formed much closer to the surface of the wing, so that the secondary separation of the boundary layer interacts with the separation of the primary vortex having a large impact on the primary vortex structure. This among other things explains also the sensitivity of the vortex flow of non-slender wings to Reynolds number effects.

In an investigation of non-slender delta wings Miau et al.[15] found out that the leading edge shape plays an important role, reinforcing the fact that the interaction between boundary layer, shear layer and vortices is large influencing the vortex generation process.

Breitsamter and Laschka[1] reveal with hot-wire velocity measurement of a delta canard configuration similar to the Eurofighter a complex vortex system consisting of wing and canard vortices. These vortices interacts differently at various canard deflections. At higher AoA the flow field is dominated by the wing leading edge vortices, where the primary vortices move inboard towards the fuselage and upwards above the wing.

Flow over a non-slender delta wing even at static conditions can have considerable unsteady contributions. Taylor et al.[17] measured velocity distributions on a $\Lambda = 50°$ delta wing and found out that for increasing AoA velocity fluctuations along the shear layer reattachment line are evident.

Gursul[4] summarizes unsteady phenomena of delta wing flows where in this context the Kelvin-Helmholtz and helical mode instabilities and the vortex breakdown oscillation have relevance. Small scale vortices around the primary vortex of the delta wing are attributed to the Kelvin-Helmholtz type instability of the shear layer. These small scale vortices can persist even after vortex breakdown of the primary vortex. The flow downstream of the vortex breakdown exhibits a hydrodynamic instability known as helical mode instability. Downstream of the vortex breakdown position are velocity and pressure fluctuations confined in an annular structure assigned to the remaining swirling vortex sheet (see Breitsamter and Laschka[2]). The dominant frequency of the helical mode instability is a function of angle of attack and wing sweep and is important for the evaluation of buffeting problems (see also Breitsamter and Laschka[2]).

Menke, Gursul, Lee at al.[4,10,13,14] investigate non-stationary phenomena in vortex breakdown location wandering of slender and non-slender delta wings at increasing AoA's. For low AoA's unsteady movement of the vortex breakdown location even to perturbations is rather small. This changes for increasing AoA's where even self-excitation of the vortex breakdown location wandering is seen. These streamwise oscillations of vortex breakdown location can have an amplitude in the order of 10% of mean chord and they are asymmetric with respect to the left and right wing half which suggests a kind of interaction between the two wing halves. There are two explanations for the interaction mechanism. Either a crossflow instability or a streamwise instability. In a crossflow instability the vortices oscillate periodically around a mean symmetric position whereas in a streamwise instability the two breakdown regions influence each other and cause periodic displacements in streamwise direction with 180° phase shift. The results of the velocity measurements point more to the streamwise instability mechanism.

Another finding is that the amplitude of oscillations increase with AoA and sweep angle when the vortices get closer to each other. The frequency range of unsteady flow phenomena on a delta wing distinguishes four regions[14], namely that of

- $0.001 < fc/U_\infty < 0.03 \rightarrow$ aerodynamic manoeuvres,
- $0.05 < fc/U_\infty < 0.1 \rightarrow$ large amplitude fluctuations of breakdown location,
- $1 < fc/U_\infty < 4 \rightarrow$ small amplitude Helical mode instability and
- $6 < fc/U_\infty < 30 \rightarrow$ small amplitude Kelvin-Helmholtz instability.

It is interesting to note in this context that the large amplitude oscillations of the vortex breakdown location take place at much smaller Strouhal numbers than usual aerodynamic phenomena. A possible relationship between large amplitude low frequency fluctuations of the vortex breakdown location and the helical mode instability was investigated by Gursul and Yang[8]. They showed that the dominant frequency of the oscillation of vortex breakdown location was much lower than the frequency of the helical mode instability. Therefore the helical mode instability has no effect on the oscillations of breakdown location.

Gursul, Vardaki et al.[5,7,19] investigate vortex breakdown movement for pitching and rolling delta wing as well as for accelerating and decelerating freestream conditions. Their findings are that an acceleration of the freestream leads from a jet like to a wake axial velocity distribution within the vortex shifting vortex breakdown location more upstream, the opposite holds for a deceleration of the freestream. The highest sensitivity to freestream dynamics is seen when vortex breakdown location is over the trailing edge. Pitching of the delta wing leads to a variation of the pressure gradients on the wing, which influences strongly vortex breakdown. Periodic oscillation of pitch angle with increasing frequency can lead to a phase lag of vortex breakdown location and pitching motion of up to 180°. An oscillating rolling motion even at low frequencies can produce coherent leading edge vortices which are not present under static conditions. Hysteresis effects become larger at higher rolling frequencies.

Recent research efforts are undertaken to take advantage from the beginning knowledge of unsteady effects over non-slender wing flow described above. Gursul et al.[6] investigates active and passive control of reattachment on various low sweep wings. Symmetric and asymmetric excitation proved well to stabilize flow on the wing with an optimum frequency of Strouhal number equal 1.

This investigation deals with non-stationary characteristics measured in rolling and yawing moment during flight testing of Eurofighter aircraft at mid to high angles of attack for various manoeuvre types. For this, flight test derived rolling and yawing moment together with AoA, AoS, flap deflections and angular rates are analysed in the frequency domain in order to locate dominant frequency contents. Since vortex breakdown location could not be measured during flight testing directly, the focus is put on the spectral content in rolling and yawing moment which correlates with oscillations in vortex breakdown positions of the complex vortex system of the aircraft. The findings will be compared with previous work of Gursul et al. described above.

3. EXPERIMENTAL SETUP

Flight test manoeuvres were flown with various Eurofighter aircrafts of the test fleet. Within this investigation manoeuvres were flown at around Ma = 0.4, a Reynolds number of $Re \approx 35 \cdot 10^6$, α_{max}-9° ≤ AoA ≤ α_{max}, where α_{max} is denoted as maximum lift AoA.

3.1. Configuration

The Eurofighter Aircraft (see Figure 1) is a long coupled delta canard configuration with a leading edge sweep of Λ = 53° and an aspect ratio of AR = 2.13. Wing span is b = 10.5 m with a mean aerodynamic chord of c = 5.772 m and a resulting wing area of S = 51.2 m².
During this investigation the leading edge flaps were fully deployed.

3.2. Flight Test Manoeuvres

The following manoeuvres were flown:

- WUT: Increasing angle of attack from trimmed Mach number condition up to target angle of attack in a slow manner at constant Mach number
- PD: After WUT to test angle of attack applying sinusoidal pitch stick input (half stick, duration approximately 1.5 sec) at test Mach number
- FRD: After WUT to test angle of attack applying sinusoidal rudder input (performed automatically initiated by flight control system, duration approximately 2 sec) at test Mach number
- FRD-Decel: Fast deceleration by chopping power setting to idle and applying full pitch stick then applying sinusoidal rudder input (performed automatically initiated by flight control system, duration approximately 2 sec) at test angle of attack and test Mach number
- R3211: After WUT to test angle of attack applying a 3-2-1-1 half roll stick input (1.5 sec / 1 sec / 0.5sec / 0.5 sec input duration in changing directions) at test Mach number
- RR: After WUT to test angle of attack applying box car type full roll stick at test Mach number
- RR-Decel: Fast deceleration by chopping power setting to idle and applying full pitch stick & full roll stick at test angle of attack and test Mach number

3.3. Signal Conditioning

All evaluated signals in this investigation such as angle of attack, angle of sideslip, flap deflections, linear and angular rates & accelerations are processed with a sampling frequency of 20Hz. The original raw data signals of the aircraft are measured with a far higher sampling rate than 20Hz. The sensors of the aircraft have an integrated, analog low-pass anti-aliasing filter, which is standard nowadays. This raw data is further digitally down-sampled to the above mentioned 20Hz by utilizing a digital low-pass anti-aliasing filter. Therefore, it can be excluded that high-frequency contributions of the signals are mapped into the low-frequency region below 20Hz, which is investigated within this paper.

4. METHODS

In this investigation the spectral content of input signals such as AoA, AoS, angular rates and flap deflections and rolling and yawing moment coefficient signals are evaluated for each manoeuvre.
To achieve this, the signals have to be treated carefully in order to obtain maximum information content. The input signals are first de-trended and shifted by a constant offset so that they have zero mean value. Then a finite Fourier transformation according to Morelli[16] is applied. The transformed values are squared and their absolute values are taken for the subsequent analysis.
The approach for the rolling and yawing moment coefficients is described below. First, Newton equations of motion are utilized in order to calculate the flight derived absolute moment coefficients

$$\frac{d}{dt}\left(\bar{\bar{I}}\vec{\omega}\right) = \vec{M}_{FT} + \vec{M}_{Nozzle} + \vec{M}_{Intake} + \vec{M}_G \quad \text{with} \tag{1}$$

$$\vec{M}_{FT} = \begin{pmatrix} c_{lFT} \cdot q \cdot S \cdot s \\ c_{mFT} \cdot q \cdot S \cdot c \\ c_{nFT} \cdot q \cdot S \cdot s \end{pmatrix}. \tag{2}$$

where the aircraft inertia $\bar{\bar{I}}$ is crudely modelled by a so-called load sheet. The load sheet is a table where the aircraft inertia is given as a function of the measured fuel content. The aircraft motion $\vec{\omega}$ is measured during flight. The intake momentum $\vec{M}_{Intake}$ and nozzle moments $\vec{M}_{Nozzle}$ of the EJ200 engines are modelled by a thrust-in-flight deck provided by Eurojet. The thrust-in-flight deck needs measured input parameters such as compressor and turbine rpm as well as pressures and temperatures. The output of the equations of motion are the inertia based moments $\vec{M}_{FT}$ around the aircraft centre of gravity that are then transformed to the aerodynamic centre of reference.
In parallel, the existing aerodynamic model (ADM) is fed by the measured parameters such as angle of attack α, angle of sideslip β, Mach number, control deflections δ etc to give predicted forces and moments around the aerodynamic reference centre (see equation 3).

$$\vec{c}_{ADM} = \begin{pmatrix} c_{lADM} \\ c_{mADM} \\ c_{nADM} \end{pmatrix} = \begin{pmatrix} \Im_l(\alpha, \beta, Ma, \delta, ...) \\ \Im_m(\alpha, \beta, Ma, \delta, ...) \\ \Im_n(\alpha, \beta, Ma, \delta, ...) \end{pmatrix} = \vec{\Im}. \tag{3}$$

The difference between predicted moment coefficients coming from the ADM and "measured" moment coefficients coming from the equations of motion is

assumed to be covered by a polynomial correction model which is shown here only for the rolling and yawing moment

$$(4)\quad c_{l,FT} - c_{l,ADM} = \Delta c_l = \sum_{i=1}^{3} c_{lpi} \cdot p^i + \sum_{i=1}^{3} c_{lri} \cdot r^i + \sum_{i=1}^{3} c_{l\beta i} \cdot \beta^i + \sum_{i=1}^{3} c_{l\xi i} \cdot \xi^i + \sum_{i=1}^{3} c_{l\zeta i} \cdot \zeta^i$$

$$(5)\quad c_{n,FT} - c_{n,ADM} = \Delta c_n = \sum_{i=1}^{3} c_{npi} \cdot p^i + \sum_{i=1}^{3} c_{nri} \cdot r^i + \sum_{i=1}^{3} c_{n\beta i} \cdot \beta^i + \sum_{i=1}^{3} c_{n\xi i} \cdot \xi^i + \sum_{i=1}^{3} c_{n\zeta i} \cdot \zeta^i$$

where the coefficients of the polynomials are determined by a least-square algorithm.
From the flight derived rolling and yawing moment coefficients the contribution of the ADM and the one of the polynomial are subtracted where additionally an offset (Δc_{l0}, Δc_{n0}) is added that guarantees zero mean value of the resulting signal.

$$(6)\quad \tilde{c}_{l,FT} = c_{l,FT} - c_{l,ADM} - \Delta c_l + \Delta c_{l0}$$

$$(7)\quad \tilde{c}_{n,FT} = c_{n,FT} - c_{n,ADM} - \Delta c_n + \Delta c_{n0}$$

The resulting signals $\tilde{c}_{l,FT}, \tilde{c}_{n,FT}$ are now nearly free from any stationary aerodynamic contribution. These signals are processed in a chirp z-transform based finite Fourier transformation according to Morelli[16], then squared. The absolute values are then presented in the subsequent figures and discussed.
The finite Fourier transformation of both the input variables and the moment coefficients requires minimum and maximum frequency and the frequency resolution. In this investigation the minimum and maximum frequency ω_0, ω_1 are defined by

(8) ω_0 = max(0.1rad/sec; $2\pi/T$) with T being the time window of the manoeuvre
(9) ω_1 = 20rad/sec < $\pi f_{sampling}$ = 62.8rad/sec with the sampling frequency of $f_{sampling}$ = 20 Hz

The above minimum and maximum frequencies lead to:

- ω_0 = 2.1rad/sec $\rightarrow f_0$ = 0.33Hz $\rightarrow f_0 c/U_\infty$ = 0.015
- ω_1 = 20rad/sec $\rightarrow f_1$ = 3.2Hz $\rightarrow f_1 c/U_\infty$ = 0.14

with T = 3sec, c = 5.772m and U_∞ = 130m/sec, just to have an orientation for the various frequency values.
The manoeuvre time slices vary between 3 sec and 8 sec which amounts to 61 to 141 data points in the time domain. For a discrete Fourier transformation the record length of the data in the time domain constrains the frequency resolution in the frequency domain. Morelli[12] proves that the chirp z-transform based finite Fourier transformation, used in this investigation, decouples the frequency resolution from the length of the time record. Therefore, the chirp z-transform based Fourier transformation is also called zoom Fourier transform. With this finite Fourier transformation, the frequency resolution can be chosen arbitrarily. In this investigation 101 evenly distributed break points were chosen within the frequency window.

5. RESULTS

In the following, the spectra of various manoeuvres types are summarized in Figure 2 to Figure 8. Here, the spectral content of input variables such as AoA, AoS, angular rates and flap deflections are shown versus the non-dimensionalized frequency fc/U_∞. Moreover, the spectral content of input variables can be compared to the spectral content of rolling and yawing moment coefficient. The input variables and moment coefficients are post-processed as shown in detail in the previous chapter.
The motivation of this approach is to show the impact of various manoeuvre excitations at increasing AoA's on the lateral-directional spectral aerodynamic characteristics.

5.1. Pitch Doublet Manoeuvre (PD)

In Figure 2 the spectral content of input variables and rolling and yawing moment coefficients is shown for three AoA's during PD type manoeuvre input. As can be expected, only the longitudinal input variables show a significant contribution. Namely AoA α, trailing edge flap δ, and pitch rate q have significant contributions up to $fc/U_\infty \approx$ 0.04.
The spectral content of rolling c_l and yawing c_n moment correlates well with the lateral-directional input variables such as AoS, p, r, ξ and ζ showing almost no contribution.

5.2. 3-2-1-1 Roll stick input (R3211)

In Figure 3 the spectral content of input variables and rolling and yawing moment coefficients is shown for four AoA's during R3211 type manoeuvre input.
In contrast to the PD results the R3211 type manoeuvre has a rich excitation of all involved input variables up to $fc/U_\infty \approx$ 0.06. But the excitation in rolling and yawing moment is relatively small, indicating only one minor peak in yawing moment c_n for highest α_{max}-1° at around $fc/U_\infty \approx$ 0.09 which is clearly above the frequency level of all the input variables.

5.3. Frequency Biased Rudder Doublet (FRD)

In Figure 4 the spectral content of input variables and rolling and yawing moment coefficients is shown for five AoA's during FRD type manoeuvre input.
The input variables show significant contributions up to $fc/U_\infty \approx$ 0.04 where AoS β, yaw rate r and rudder deflection ζ show a characteristic contribution at $fc/U_\infty \approx$ 0.025 reflecting the frequency of the sinusoidal input of the rudder and the resulting aircraft motion.
The spectral content of rolling moment show only minor peaks for the highest AoAs at α_{max}-1°, $fc/U_\infty \approx$ 0.075 and α_{max}, $fc/U_\infty \approx$ 0.09. In contrast to this, the yawing moment c_n spectrum shows larger peaks for α_{max}-1° at 0.06 < fc/U_∞ < 0.11 and for α_{max} at 0.07 < fc/U_∞ < 0.14 far beyond the frequency level of the input variables.

5.4. Rapid Roll (RR)

Figure 5 and Figure 6 summarize the spectral content of the clockwise and counter-clockwise flown RR type manoeuvres for three AoA's. The spectral content of the input variables for both rolling directions is concentrated in

the range of fc/U_∞ < 0.04 where naturally the roll p and aileron ξ excitation show large values.
It can be seen that the corresponding spectral content of rolling and yawing moment increases with AoA and shows significant peaks in the range of 0.02 < fc/U_∞ < 0.12 for c_l and c_n. The low frequency content correlates with the input variable based excitation (fc/U_∞ < 0.04) but the most significant part of the spectral content resides beyond the input value frequencies at around 0.055 < fc/U_∞ < 0.09.
Furthermore, it is interesting to note that the peaks of the spectra are different for clockwise and counter-clockwise turn indicating a well known asymmetry of the aircraft geometry between left and right wing (gun blister at starboard wing apex).

5.5. Frequency Biased Rudder Doublet under Deceleration and Pitch-up (FRD-Decel)

In Figure 7 the spectral content of input variables and rolling and yawing moment coefficients is shown during a FRD-Decel type manoeuvre input at α_{max}.
The spectral content of the input variables is contained within fc/U_∞ < 0.04. Most remarkable is the clear peak in the rolling moment spectral content at 0.06 < fc/U_∞ < 0.075 which has no comparable pendant in the yawing moment spectrum. The yawing moment show small peaks distributed across the whole investigated frequency range with some contributions at 0.05 < fc/U_∞ < 0.1.

5.6. Rapid Rolling under Deceleration and Pitch-up (RR-Decel)

In Figure 8 the spectral content of input variables and rolling and yawing moment coefficients is shown for three RR-Decel type manoeuvre inputs where the manoeuvres were flown with increasing excitation level from No.1 to No.3 at α_{max}.
Input variable spectral content is concentrated within fc/U_∞ < 0.04 which seems to be a characteristic boundary for the flight mechanical frequency excitation.
Manoeuvre No.1 shows a clear excitation in the rolling moment c_l at the boundary of input variable excitation $fc/U_\infty \approx$ 0.04 and further two peaks at $fc/U_\infty \approx$ 0.06 and $fc/U_\infty \approx$ 0.1. In the yawing moment c_n, there are also two distinct peaks at $fc/U_\infty \approx$ 0.07 and 0.09.
Manoeuvre No.2 has a similar peak distribution in the rolling moment c_l as No.1, namely at $fc/U_\infty \approx$ 0.04 and 0.08. In the yawing moment c_n significant spectral contributions are at 0.035 < fc/U_∞ < 0.05 and 0.07 < fc/U_∞ < 0.09.
Manoeuvre No.3 has a clear excitation in the rolling moment c_l at 0.04 < fc/U_∞ < 0.06 and in the yawing moment c_n at 0.03 < fc/U_∞ < 0.045 and 0.07 < fc/U_∞ < 0.09.
All RR-Decel type manoeuvres have clear excitation in the rolling and yawing moment starting there where the input variable excitation stops and reaching up to $fc/U_\infty \approx$ 0.09.

6. DISCUSSION

The results shown in the previous chapter show clearly the influence of AoA and manoeuvre type on the spectral content of the rolling and yawing moment.
For a longitudinal manoeuvre no relevant oscillation of rolling and yawing moment can be achieved at all, at least up to maximum lift AoA. For a R3211 and FRD type manoeuvre rolling and yawing moment excitation starts just below maximum lift AoA = α_{max}-1°. A rapid rolling manoeuvre excites rolling and yawing moment even at lower AoA = α_{max}-3°. A deceleration and pitch up during FRD or RR changes spectral characteristics in rolling and yawing moment where for a FRD-Decel major oscillations shift from the yawing moment to the rolling moment during deceleration and dynamic pitch-up.
Major spectral content in rolling and yawing moment can be found in the range of 0.04 < fc/U_∞ < 0.14 which is the typical frequency range of large amplitude vortex breakdown oscillation[4-8,10,13,14], where the amplitude of oscillations depends on the manoeuvre type.
Moreover, for all manoeuvres the spectral content of the input variables is concentrated mainly up to fc/U_∞ < 0.04, therefore excluding a direct excitation of the spectral content of vortex breakdown location fluctuation and of the rolling and yawing moments due to the excitation of the input variables. Furthermore, Gursul and Yang[8] exclude the possibility that oscillations in the low frequency range (0.04 < fc/U_∞ < 0.14) may be influenced by helical mode instabilities.
Thus, the driving force behind the oscillations in rolling and yawing moment are fluctuations in vortex breakdown position be it in streamwise or spanwise direction of the complicated vortex system of the aircraft. This results in changes in vortex circulation influencing vortex lift and drag that sum up to forces and moment around the aircraft. Therefore a correlation can be drawn between oscillation and spectral content of rolling & yawing moment and vortex breakdown location fluctuation.
The structure of the spectra is complicated and multifaceted/multipeaked pointing to a multi modal three-dimensional movement of the various vortices coming from the canard and wing leading edge and their breakdown locations on the wing.
In spite of the complicated configuration and experimental conditions compared to previous wind-tunnel investigations with more simple models the results in this investigation can be seen as a continuation of preceding work of Gursul et al.[4-8,10,13,14], confirming the results with slender and non-slender delta wings.
The results presented in this investigation have also practical relevance since it becomes clear that oscillations in the vortex breakdown location on the delta wing near maximum lift AoA are highly probable and can achieve amplitudes for rolling and yawing moment coefficients of up to 20% of their maximum values. Although this may pose no harm for the safety of the aircraft it may change handling characteristics compared to the mid and low AoA range. Furthermore, issues such as aerodynamic model validation must also account for these non-stationary issues, at least in form of tolerances. Thus, it must be taken care that unsteady effects are not modelled by additional static correction terms inefficiently and in a wrong manner.

7. CONCLUSION

This investigation deals with non-stationary effects in rolling and yawing moment just below and at maximum lift AoA for the Eurofighter aircraft, which is a delta-canard configuration. Spectral analysis of AoA, AoS, angular rates, flap deflections and rolling & yawing moment is performed where oscillations and the spectral content of

rolling and yawing moment in the range of $0.04 < fc/U_\infty < 0.14$ point to fluctuations of vortex breakdown location.
For all manoeuvres, the spectral content of the input variables (AoA, AoS, angular rates, flap deflections) is concentrated mainly up to $fc/U_\infty < 0.04$, therefore excluding a direct excitation of the spectral content of vortex breakdown location fluctuation and of the rolling and yawing moments due to the excitation of the input variables.
Previous work of Gursul et al. on asymmetric oscillations of vortex breakdown location for slender and non-slender delta wings are confirmed. Fluctuations in the vortex breakdown location are reported to take place in a frequency range of around $0.05 < fc/U_\infty < 0.1$ which is far lower compared to the frequency range for helical mode or Kelvin-Helmholtz instabilities. It can be shown in this investigation that the relevant frequency range of $0.04 < fc/U_\infty < 0.14$ for rolling and yawing moment oscillations coincides with the frequency range of large amplitude fluctuations of breakdown location reported by Gursul et al. where the amplitude of oscillations depends on the manoeuvre type.
In contrast to previous work of Gursul, the structure of spectral content of rolling and yawing moment in this frequency range is rather complicated and multifaceted/multipeaked pointing to a multi modal three-dimensional movement of the various vortices of canard and wing leading edge and their breakdown locations on the wing.

8. REFERENCES

[1] Breitsamter, C., Laschka, B., Velocity Measurements with Hot-Wires in a Vortex Dominated Flowfield, AGARD Conference Proceeding 535-11, presented at an AGARD Meeting on "Wall Interference, Support Interference and Flow Field Measurements", Oct. 1993

[2] Breitsamter, C., Laschka, B., Aerodynamic Active Control for EF-2000 Fin Buffet Load Alleviation, AIAA-2000-0656, 38th Aerospace Sciences Meeting & Exhibit, Jan. 2000, Reno

[3] Elsayed, M., Scarano, F., Verhaagen, N., G., Leading Edge Shape Effect on the Flow over Non-Slender Delta Wings, AIAA-2008-0344, 46th Aerospace Meeting Sciences Meeting & Exhibit, Jan. 2002, Reno

[4] Gursul, I., Review of Unsteady Vortex Flows over Delta Wings, AIAA-2003-3942, 21st Applied Aerodynamics Conference, Orlando, Jun. 2003

[5] Gursul, I., Ho, C., M., Vortex Breakdown over Delta Wings in Unsteady Free Stream, AIAA-1993-0555, 31st Aerospace Sciences Meeting and Exhibit, Reno, Jan. 1993

[6] Gursul, I., Vardaki, E., Wang, Z., Active and Passive Control of Reattachment on Various Low-Sweep Wings, AIAA-2006-0506, 44th Aerospace Sciences Meeting and Exhibit, Reno, Jan. 2006

[7] Gursul, I., Yang, H., Vortex Breakdown over a Pitching Delta Wing, AIAA-1994-0536, 32nd Aerospace Sciences Meeting and Exhibit, Reno, Jan. 1994

[8] Gursul, I., Yang, H., On Fluctuations of Vortex Breakdown Location, Physics of Fluids, Vol. 7, No. 1, 1995, pp. 229-231

[9] Hummel, D., On the Vortex Formation over a Slender Wing at Large Angles of Incidence, AGARD-CP-494, pp. 15-1 to 15-17, Jul. 1991

[10] Lee, Y., L., Gursul, I., An Investigation of Unsteady Interactions of a Vortex Pair over Delta Wings, AIAA-2003-0423, 41st Aerospace Sciences Meeting and Exhibit, Reno, Jan. 2003

[11] Luckring, J., M., Reynolds Number and Leading Edge Bluntness Effects on a 65° Delta Wing, AIAA-2002-0419, 40th Aerospace Meeting Sciences Meeting & Exhibit, Jan. 2002, Reno

[12] Luckring, J., M., Initial Experiments and Analysis of Blunt-Edge Vortex Flows, AIAA-2008-0378, 46th Aerospace Meeting Sciences Meeting & Exhibit, Jan. 2002, Reno

[13] Menke, M., Gursul, I., Self-Excited Oscillations of Vortex Breakdown Location over Delta Wings, AIAA-1997-0744, 35th Aerospace Sciences Meeting and Exhibit, Reno, Jan. 1997

[14] Menke, M., Yang, H., Gursul, I., Further Experiments on Fluctuations of Vortex Breakdown Location, AIAA-1996-0205, 34th Aerospace Sciences Meeting and Exhibit, Reno, Jan. 1996

[15] Miau, J., J., Kuo, K., T., Liu, W., H., et al., Flow Developments Above 50-Deg Sweep Delta Wings with Different Leading-Edge Profiles, Journal of Aircraft, Vol. 32, No. 4, Jul.-Aug. 1995

[16] Morelli, E., High Accuracy Evaluation of the Finite Fourier Transform Using Sampled Data, NASA TM-110340, Jun. 1997

[17] Taylor, G., S., Gursul, I., Unsteady Vortex Flows and Buffeting of a Low Sweep Delta Wing, AIAA-2004-1066, 42nd Aerospace Sciences Meeting and Exhibit, Reno, Jan. 2004

[18] Taylor, G.,S., Schnorbus, T., Gursul, I., An Investigation of Vortex Flows over Low Sweep Delta Wings, AIAA-2003-4021, 33rd AIAA Fluid Dynamics Conference and Exhibit, Florida, Jun. 2003

[19] Vardaki, E., Gursul, I., Vortex Flows on a Rolling Nonslender Delta Wing, AIAA-2004-4729, 22nd Applied Aeodynamics Conference and Exhibit, Rhode Island, Aug. 2004

9. FIGURES

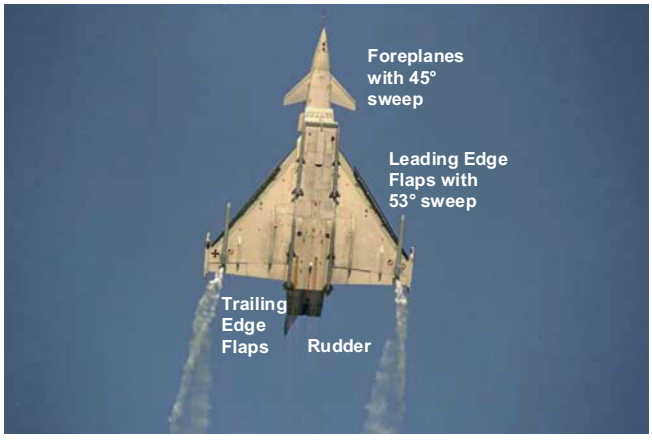

Figure 1. Eurofighter aircraft

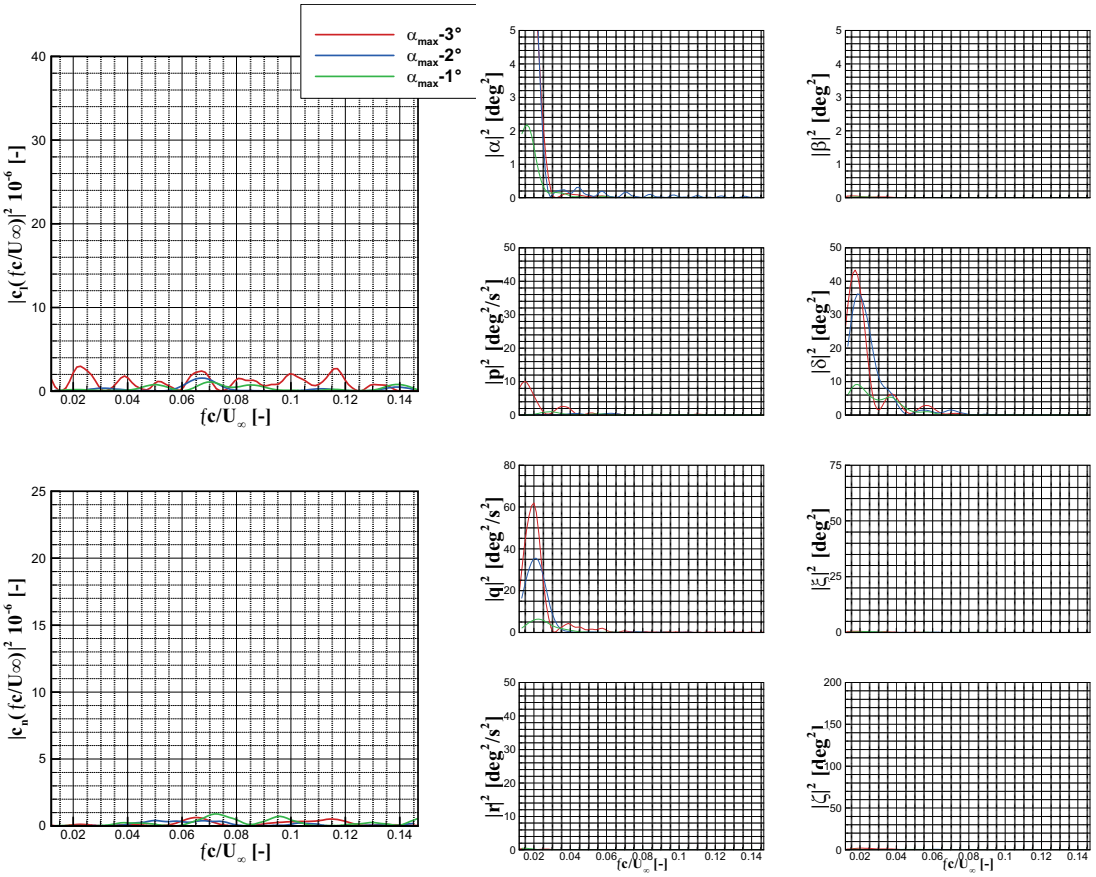

Figure 2. Spectral Content of input, rolling and yawing moment signal for PD's at increasing AoA

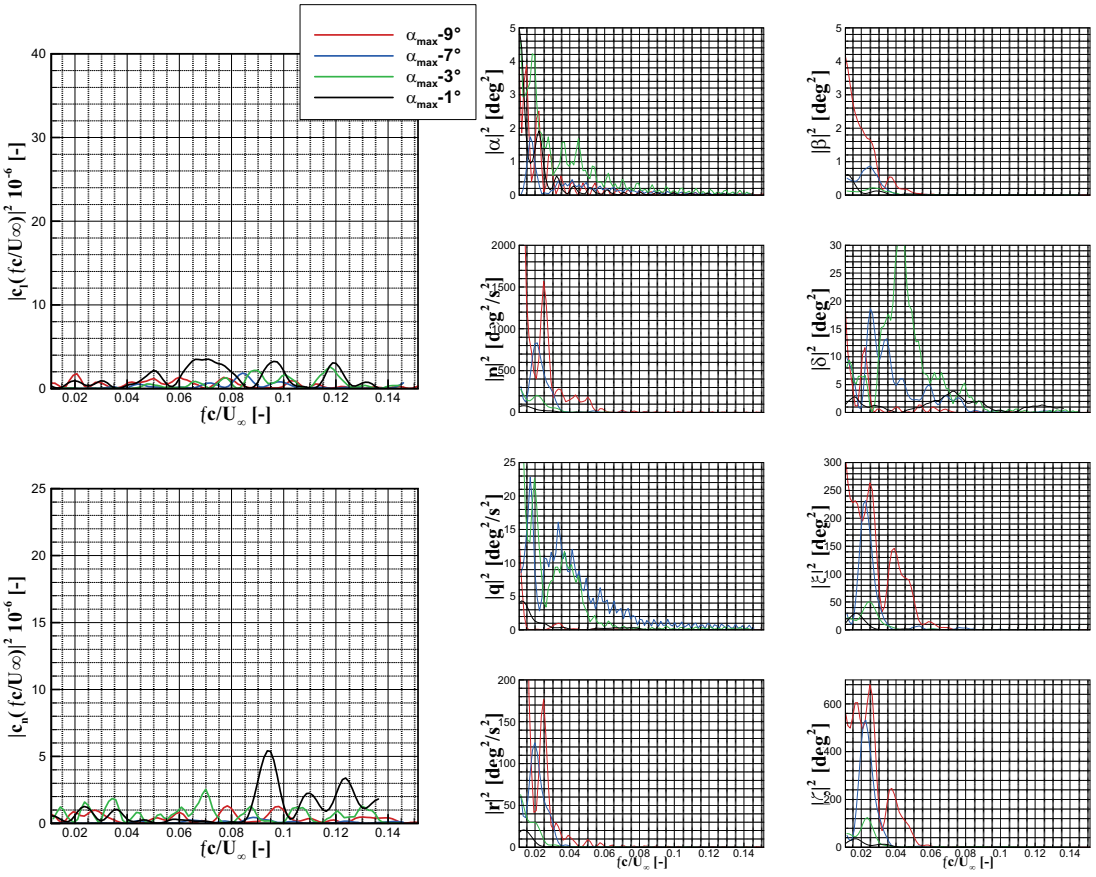

Figure 3. Spectral Content of input, rolling and yawing moment signal for R3211's at increasing AoA

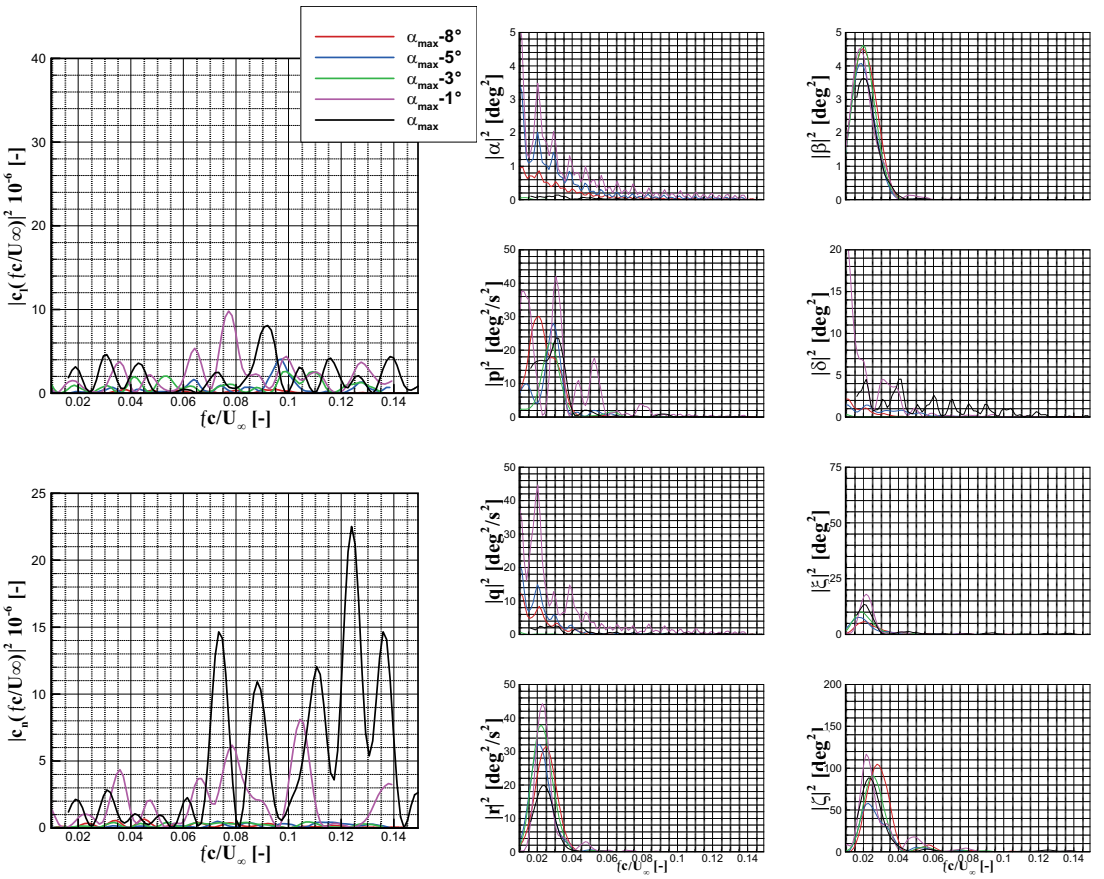

Figure 4. Spectral Content of input, rolling and yawing moment signal for FRD's at increasing AoA

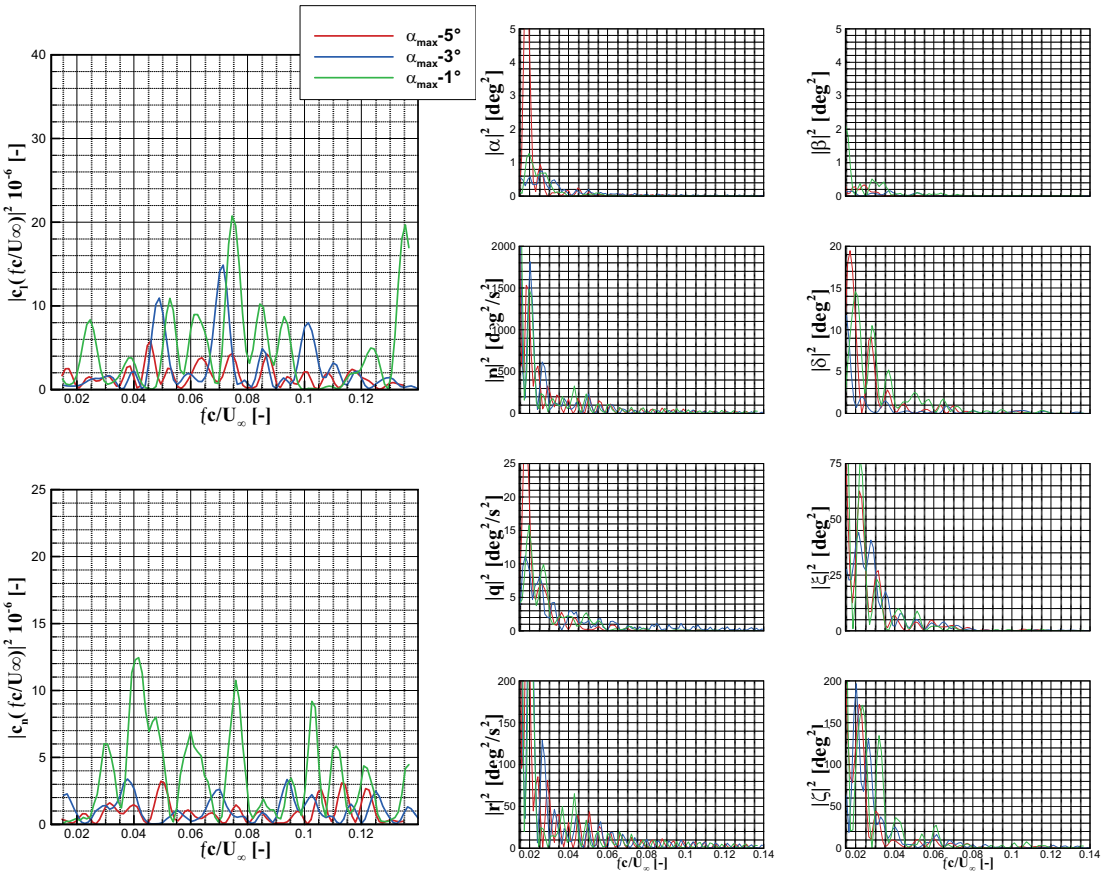

Figure 5. Spectral Content of input, rolling and yawing moment signal for clockwise RR's at increasing AoA

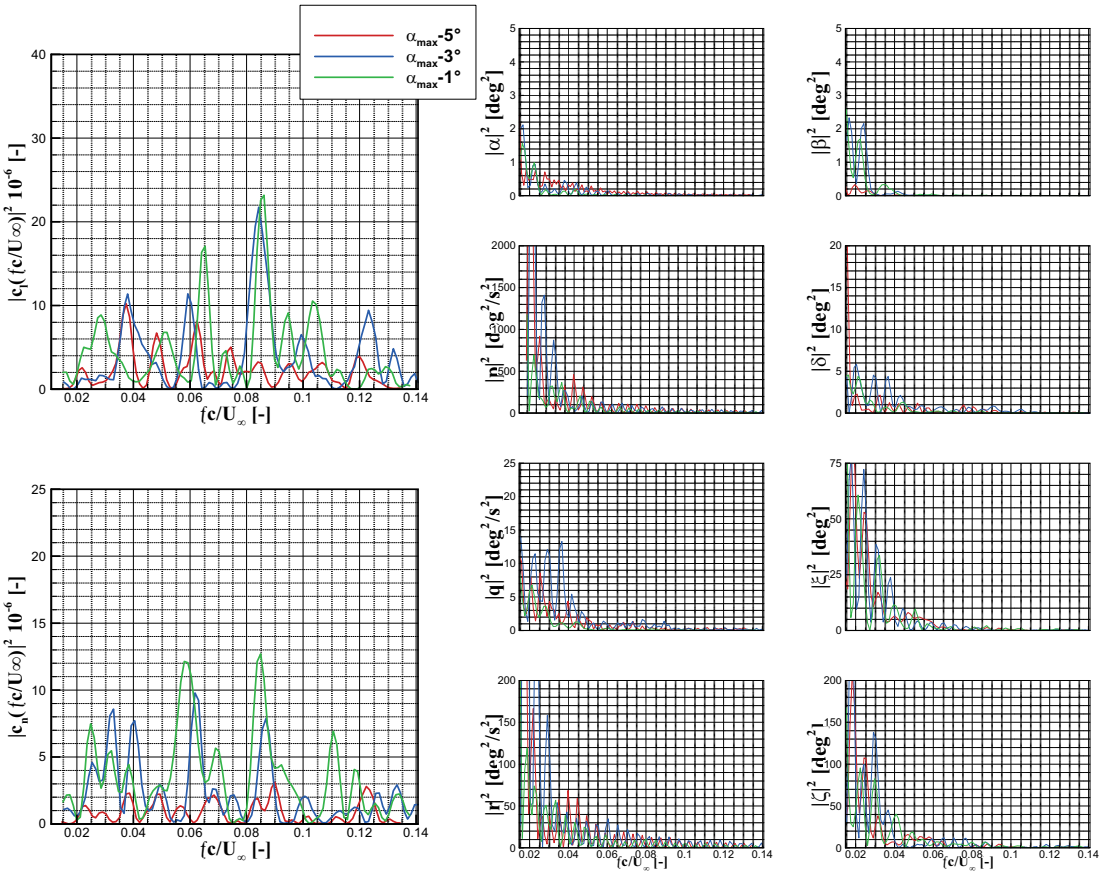

Figure 6. Spectral Content of input, rolling and yawing moment signal for counter-clockwise RR's at increasing AoA

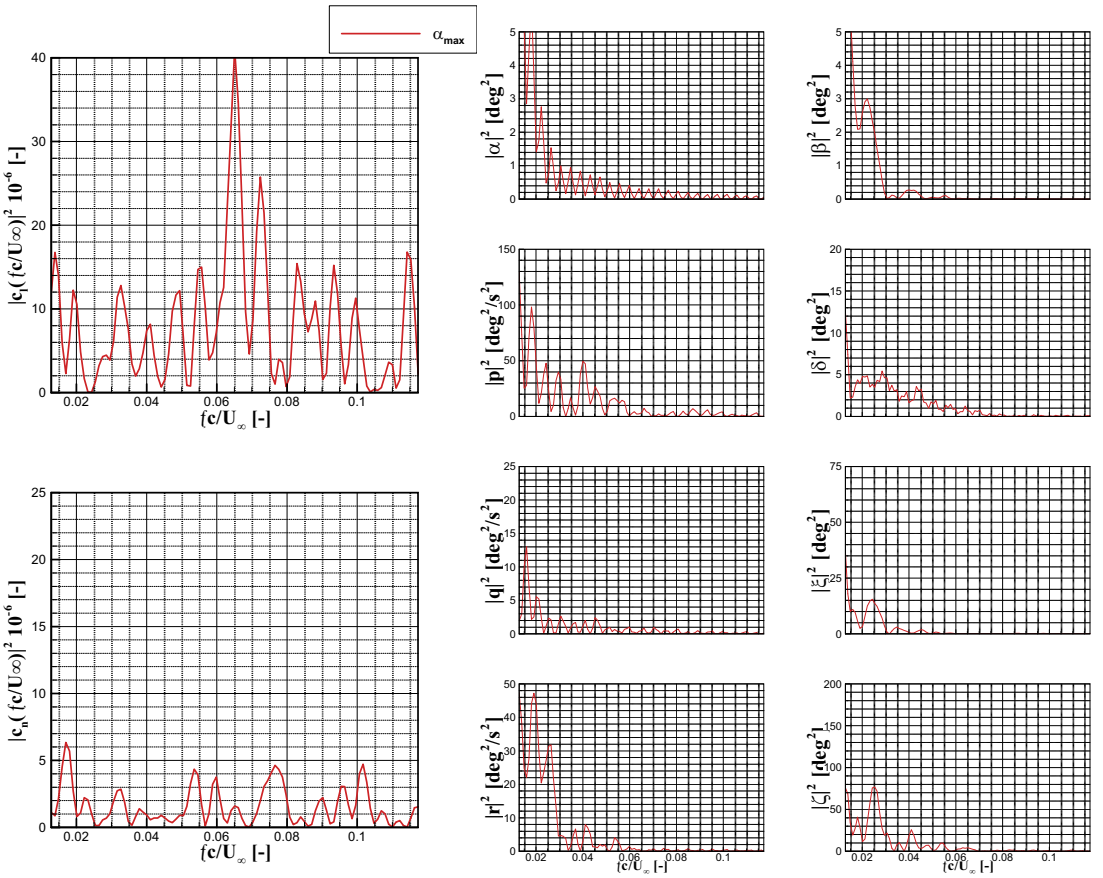

Figure 7. Spectral Content of input, rolling and yawing moment signal for FRD-Decel at α_{max}

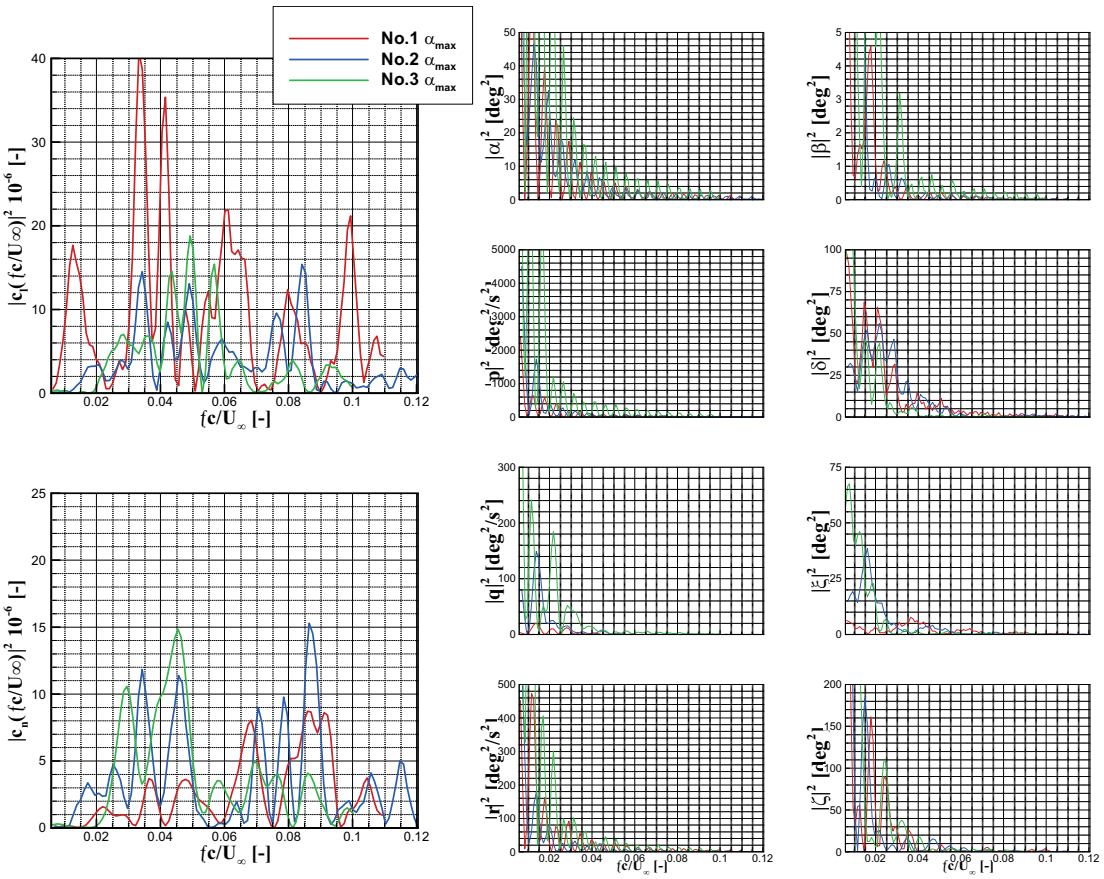

Figure 8. Spectral Content of input, rolling and yawing moment signal for RR-Decel at α_{max} for increasing manoeuvre excitation from No.1 to No.3